ISSN 1063-7761, Journal of Experimental and Theoretical Physics, 2006, Vol. 103, No. 6, pp. 904–916. © Pleiades Publishing, Inc., 2006.
Original Russian Text © V.E. Zobov, A.A. Lundin, 2006, published in Zhurnal Éksperimental'noĭ i Teoreticheskoĭ Fiziki, 2006, Vol. 130, No. 6, pp. 1047–1060.

STATISTICAL, NONLINEAR, AND SOFT MATTER PHYSICS

Second Moment of Multiple-Quantum NMR and a Time-Dependent Growth of the Number of Multispin Correlations in Solids

V. E. Zobov[a] and A. A. Lundin[b]

[a] *Kirenskiĭ Institute of Physics, Siberian Division, Russian Academy of Sciences, Krasnoyarsk, 660036 Russia*
e-mail: rsa@iph.krasn.ru

[b] *Semenov Institute of Chemical Physics, Russian Academy of Sciences, Moscow, 117977 Russia*
e-mail: andylun@orc.ru

Received March 6, 2006

Abstract—The time evolution of multispin correlations (the growth of the number of correlated spins as a function of time) can be observed directly using the multiple-quantum nuclear magnetic resonance spectroscopy of solids. A quantity related to this number, namely, the second moment $\langle n^2(t)\rangle$ of the intensity distribution of coherences of different orders in the multiple-quantum spectrum can be calculated using the theory proposed in this work. An approach to the calculation of the four-spin time correlation function through which this moment is expressed is developed. The main sequences of contributions in the expansion of this function into a time power series are summed using the approximation of a large number of neighbors both for systems with a secular dipole–dipole interaction and for systems with a nonsecular effective interaction. An exponential dependence of $\langle n^2(t)\rangle$ is obtained. The value of $\langle n^2(t)\rangle$ is additionally calculated using an expansion in terms of orthogonal operators for three model examples corresponding to different limiting realizations of spin systems. It is shown that the results of the microscopic theory at least qualitatively agree with both the results obtained for model examples and experimental results obtained recently for adamantane.

PACS numbers: 76.60.-k, 76.60.Es, 75.20.Ck

DOI: 10.1134/S1063776106120089

1. INTRODUCTION

Theoretical studies of an increase in the number of particles involved in a correlated motion in the course of time evolution started in the statistical physics of nonequilibrium processes many decades ago in the works on studying the dynamics of correlations by the I. Prigogin's Brussels school [1]. The recent development of experimental methods has opened up the possibility of experimentally studying the time evolution of multispin correlations by means of the observation of multiple-quantum coherences using multiple-quantum nuclear magnetic resonance (NMR) spectroscopy (see, for example, [2–10]). Unfortunately, these methods have been so far of main practical use only in studying clusters and local structures, when the multiple-quantum spectrum is rather simply understood. At the same time, the main computational algorithms are now implemented for small systems, in which control of multiple-quantum coherences is investigated with the aim to use the latter in quantum computing [11, 12]. Theoretical results can be obtained for small systems by means of numerical calculations. Radically different theoretical approaches are required for studying large systems (experimental results have been published for systems containing up to 650 correlated spins [9]), which are of interest (as distinct from small model ones) to statistical physics and quantum computing. At last, the absence of a correct theory to interpret the results constrains the application of these methods to studying common solids.

It is known that the whole diversity of particular methods of multiple-quantum Fourier spectroscopy [2–9] is reduced to the following scheme. By means of irradiating the spin system with a sequence of radio-frequency pulses, the Hamiltonian of its spin–spin interactions is transformed to a nonsecular (with respect to equilibrium magnetization) Hamiltonian, under the action of which the initial magnetization is transferred to various correlation functions of products of various numbers (K) of spin operators (multispin correlations). In other words, an equilibrium density matrix ρ_{eq} in a strong magnetic field is transformed into a nonequilibrium density matrix, which is conveniently presented as a sum of off-diagonal elements ρ_n with a certain difference n of magnetic quantum numbers that have been

called multiple-quantum coherences (n is the coherence order)

$$\rho(t) = \exp(iHt)\rho_{eq}\exp(-iHt) = \sum_n \rho_n(t),$$

$$\rho_n(t) = \sum_{K=n}^{K=N}\sum_p g_{Knp}(t)|Knp\rangle.$$

Here, $|Knp\rangle$ is a basis operator, in which K single-spin operators form a product coupling Zeeman states that differ by n units; index p numbers different basis states with the same values of K and n; and N is the total number of spins in the system. The occurring coherences are marked with the phase shift φ proportional to time. The arising phase shift is proportional to $n\varphi$, where n is an integer number. Thus, K-spin coherences, depending on n, are also distinguished by the number of quanta ($n \le K$) [2–4]. Then, a new pulse sequence changing the sign of the above nonsecular Hamiltonian is applied to the system and, thus, "time reversal" is performed [2, 13, 14], because of which the system evolves back. The one-dimensional or two-dimensional Fourier spectrum can be constructed from the observed time dependence of the evolution and phase φ.

In conventional multiple-quantum experiments, K-spin correlations are marked with a phase shift about the z axis, that is, are classified by the number of quanta in the basis in which the z components of spin operators are diagonal (from here on, the z basis). However, as was shown in [8], these correlations can also be marked with a phase shift arising upon a rotation about another axes, for example, x. Such experiments allowed additional information to be obtained already in the case of the nonsecular effective Hamiltonian. It is especially important that spin dynamics under the action of a Hamiltonian conserving z projections can be studied using measurements of coherences in a basis differing from the conventional z basis. In this way, multispin dynamics due to the secular part of the dipole–dipole interaction was observed in the x basis in [10] in the process of solid-state NMR free induction decay (FID). In all bases, a qualitatively similar pattern of the time evolution of multispin correlations was observed. This is not surprising, because this evolution is governed by the general laws of nonequilibrium statistical physics.

The time dependences of multiple-quantum-coherence amplitudes are the most important characteristics of multiple-quantum NMR spectroscopy, which are necessary both for applied (for example, structural) studies and for an understanding of the physics of irreversible processes. In their turn, these dependences determine the intensity distributions for coherences of different orders in the multiple-quantum spectrum. Based on the simplest statistical model [2, 3], a Gaussian shape is assumed in the experiment for the distribution of coherences of different orders in the multiple-quantum spectrum

$$g_n(\tau) \propto \mathrm{Tr}\{\rho_n(\tau)\rho_{-n}(\tau)\} \propto \exp\left(-\frac{n^2}{N(\tau)}\right). \quad (1)$$

The variance of the distribution in this model ($N(\tau)/2$) is determined by the number of spins $N(\tau)$ among which dynamical correlation due to the dipole–dipole interaction is settled during the preparation time τ. This number, called the number of correlated spins or the effective cluster size, grows as the preparation time τ increases. In the statistical model [2, 3], it is assumed in particular that all coherences have equal amplitudes at infinitely long τ. At the same time, the dependences observed experimentally are as a rule not described by relationship (1) (see, for example, [6]). In this connection, the necessity arises of at least replacing $N(\tau)$ with a quantity similar in its sense but resulting from first principles and independent of the model.

The second moment $\langle n^2(\tau)\rangle$ of the intensity distribution for coherences of different orders in the multiple-quantum spectrum can serve as such a quantity [15]. In the case of a Gaussian distribution, this moment coincides with the variance ($N(\tau)/2$) in (1). For the distribution of a different shape, it will also serve as a characteristic of the number of correlated spins (the effective cluster size). Although the equation relating the above moment with the correlation function of the product of four spin operators taken at different instants of time was derived by Khitrin as long ago as 1997 [15], such correlation functions have not been calculated so far.

In this paper, a theory is developed for the direct calculation of the second moment $\langle n^2(\tau)\rangle$ of the intensity distribution for coherences of different orders in a multiple-quantum NMR spectrum. To calculate considerably more complicated four-spin correlation functions, we will elaborate methods and approaches developed in our previous work and successfully applied to the calculation of two-spin time correlation functions (TCFs), which determine the shape of an ordinary single-quantum NMR absorption spectrum. Spin systems described by the Hamiltonian of the secular part of the dipole–dipole interaction and by the nonsecular effective Hamiltonian used in multiple-quantum NMR spectroscopy will be considered. Both sorts of systems are studied experimentally and are important for practice.

The paper is organized as follows. In Section 2, general equations for the second moment are considered. In Section 3, time-dependent spin-projection operators in the four-spin correlation function for $\langle n^2(\tau)\rangle$ are presented as expansions in terms of the complete system of orthonormal operators and calculations are performed for three model examples corresponding to different limiting implementations of spin systems. In Section 4, the main sequences of contributions (diagrams) in the expansion of the four-spin correlation function in terms of powers of time are selected and summed. In the last

sections, the results obtained by the two methods are compared to each other and to experimental results.

2. SECOND MOMENT OF THE INTENSITY DISTRIBUTION FOR COHERENCES OF DIFFERENT ORDERS IN A MULTIPLE-QUANTUM SPECTRUM

It is known [16] that the secular part of the internuclear dipole–dipole interaction is the main reason for the broadening of an NMR absorption spectrum in nonmetallic diamagnetic solids and, thus, completely determines the dynamics of the nuclear spin system

$$\begin{aligned} H_d &= \sum_{i\neq j} b_{ij} S_{zi} S_{zj} + \sum_{i\neq j} a_{ij} S_{+i} S_{-j} = H_{zz} + H_{ff} \\ &= \sum_{i\neq j} b_{ij} S_{zi} S_{zj} + \sum_{i\neq j} a_{ij} (S_{xi} S_{xj} + S_{yi} S_{yj}) \\ &= \sum_{i\neq j} (H_{dij}^{zz} + H_{dij}^{xx} + H_{dij}^{yy}), \end{aligned} \tag{2}$$

where

$$b_{ij} = \frac{\gamma^2 \hbar (1 - 3\cos^2 \theta_{ij})}{2 r_{ij}^3}, \quad a_{ij} = -\frac{b_{ij}}{2},$$

$\mathbf{r}_{ij}$ is the vector connecting spins i and j, θ_{ij} is the angle formed by vector $\mathbf{r}_{ij}$ and the external constant magnetic field, and $S_{\alpha i}$ is the α component ($\alpha = x, y, z$) of the vector spin operator at site i. From here on, the energy is expressed in frequency units.

The Hamiltonian (2) is the basic one for "spin alchemy" and is transformed under the action of radiofrequency pulses into other Hamiltonians being of interest to a researcher [17]. For example, the effective Hamiltonian

$$\begin{aligned} H_{\text{eff}} &= \sum_{i\neq j} c_{ij} (S_{zi} S_{zj} - S_{yi} S_{yj}) \\ &= \sum_{i\neq j} (H_{dij}^{zz}/2 + H_{dij}^{yy}) \end{aligned} \tag{3}$$

is prepared in conventional NMR spectroscopy [2–4]. Here, as distinct from the original works, the designation $c_{ij} = b_{ij}/2$ is introduced and a cyclic permutation of spin projections is performed for the convenience of further studying. The intensities of coherences of different orders in a multiple-quantum spectrum have recently been measured in [10] as functions of time for a system with the conventional secular dipole–dipole Hamiltonian (2). It has been shown that the behavior of systems described by the Hamiltonians (2) and (3) qualitatively coincides. The cyclic permutation in Eq. (3) makes the theoretical description of both cases as close as possible.

The intensity of multiple-quantum coherences observed experimentally is determined by the TCF

$$\begin{aligned} &\Gamma_\varphi(t, \tau) \\ &= \frac{1}{\mathrm{Tr} S_x^2} \mathrm{Tr}\{ U^+(\tau) U_\varphi U(t) S_x U^+(t) U_\varphi^+ U(\tau) S_x \}. \end{aligned} \tag{4}$$

Here, $U(t)$ is the evolution operator with the internal interaction Hamiltonian H_d from Eq. (2) (or this interaction transformed by radiofrequency pulses into a certain new nonsecular effective Hamiltonian H_{eff} (3)), $U_\varphi = \exp(i\varphi S_x)$ is the rotation operator by an angle φ about the x axis, and $S_x = \sum_i S_{xi}$ is the x component of the total spin of the nuclear system. For the use in the microscopic theory considered in Section 4, we introduced the designation τ for the evolution with "time reversal." Experimental conditions $t = \tau$ will be fulfilled in the final equations.

The intensity of the nth-order coherence is obtained from Eq. (4) after the Fourier transformation (integration over the variable $n\varphi$). However, as shown in [15], in order to find the second moment of the intensity distribution for coherences of different orders in a multiple-quantum spectrum, this transformation can be avoided and the following equation can be used instead:

$$\begin{aligned} \langle n^2(t) \rangle &= -\left. \frac{d^2 \Gamma_\varphi(t, t)}{d\varphi^2} \right|_{\varphi = 0} = -\frac{\mathrm{Tr}\{[S_x, S_x(t)]^2\}}{\mathrm{Tr}\{S_x^2\}}, \\ S_x(t) &= U(t) S_x U^+(t). \end{aligned} \tag{5}$$

This equation can easily be generalized to the case of $t \neq \tau$

$$\langle \langle n^2(t, \tau) \rangle \rangle = \frac{\langle n^2(t, \tau) \rangle}{2} + \frac{\langle n^2(\tau, t) \rangle}{2}, \tag{6}$$

$$\begin{aligned} \langle n^2(t, \tau) \rangle = 2 \sum_{i, j, f, q} \Bigg[&\frac{\mathrm{Tr}\{S_{xi} S_{xf} S_{xj}(t) S_{xq}(\tau)\}}{\mathrm{Tr}\{S_x^2\}} \\ &- \frac{\mathrm{Tr}\{S_{xj} S_{xi}(t) S_{xf} S_{xq}(\tau)\}}{\mathrm{Tr}\{S_x^2\}} \Bigg]. \end{aligned} \tag{7}$$

At $t = \tau$, we obtain

$$\langle \langle n^2(t, t) \rangle \rangle = \langle n^2(t, t) \rangle = \langle n^2(t) \rangle.$$

At $t \neq \tau$, the quantity $\langle n^2(t, \tau) \rangle$ contains an imaginary part vanishing in Eq. (6) after symmetrization.

The second term in the right-hand part of Eq. (7) can be rewritten as

$$\frac{\mathrm{Tr}\{S_{xj}(4S_{xf}S_{xf})S_{xi}(t)S_{xf}S_{xq}(\tau)\}}{\mathrm{Tr}\{S_x^2\}}$$

$$= \frac{\mathrm{Tr}\{S_{xj}S_{xf}\sigma_{xf}S_{xi}(t)\sigma_{xf}S_{xq}(\tau)\}}{\mathrm{Tr}\{S_x^2\}}$$

$$= \frac{\mathrm{Tr}\{S_{xj}S_{xf}\overline{S_{xi}(t)}^{(f)}S_{xq}(\tau)\}}{\mathrm{Tr}\{S_x^2\}},$$

because $4S_{xf}S_{xf} = 1$. The Pauli matrices σ_{xf} correspond to the rotation operator of the spin with the number f about the x axis by 180°. The symbol $\overline{S_{xj}(t)}^{(f)}$ means that spin f is flipped in the time evolution operator in the Hamiltonian; that is, the Hamiltonian $\sigma_{xf}H\sigma_{xf}$, in which H_{dfj}^{zz} and H_{dfj}^{yy} are replaced by $-H_{dfj}^{zz}$ and $-H_{dfj}^{yy}$, respectively, stays now in the brackets. Thus, from Eq. (7), we obtain

$$\langle n^2(t,\tau)\rangle = 2\sum_{i,j,f,q}\frac{1}{\mathrm{Tr}\{S_x^2\}} \times \mathrm{Sp}\{S_{xj}S_{xf}(S_{xi}(t) - \overline{S_{xi}(t)}^{(f)})S_{xq}(\tau)\}. \quad (8)$$

3. GROWTH OF THE SECOND MOMENT OF A MULTIPLE-QUANTUM SPECTRUM AND AMPLITUDES OF ORTHOGONAL OPERATORS

The direct calculation of the four-spin TCFs in Eq. (5) or (8) is a very complicated task, to which we will return in Section 4. The dependence of $\langle n^2(t)\rangle$ on the properties of the expansion amplitudes $S_x(t)$ in terms of the complete system of orthonormal operators [18–23]

$$S_x(t) = \sum_{j=0}^{\infty} A_j(t)|j\rangle \quad (9)$$

is studied in this section below.

Many works are devoted to studying such expansions in nonequilibrium statistical mechanics (see, for example, [18–23]).

The expansion in terms of orthogonal operators given in the Introduction has already been used previously in the calculations of the amplitudes of multiple-quantum coherences [2–9]. However, different bases are taken in the equation in the Introduction and in Eq. (9). In the Introduction, the universal basis is formed by all possible products of different spin-projection operators of the system. This is convenient for calculations of small clusters. As the number K of single-spin operators increases, the number of basis operators increases by an exponential law. To overcome mathematical difficulties, authors have to introduce uncontrolled approximations, for example, by replacing the exact equations of motion with the random-walk equations in the Liouville space. At the same time, a basis constructed for a particular Hamiltonian and the initial operator $|0\rangle = S_x$ rather than the universal basis is used in Eq. (9). Each subsequent operator of the basis is obtained from the preceding one after the calculation of the commutator with the Hamiltonian according to the recurrence equation

$$|1\rangle = i[H, |0\rangle],$$
$$|k+1\rangle = i[H, |k\rangle] + \nu_{k-1}^2|k-1\rangle, \quad k \geq 1,$$
$$\nu_k^2 = \frac{\mathrm{Tr}\{\langle k+1|k+1\rangle\}}{\mathrm{Tr}\{\langle k|k\rangle\}}.$$

Note that, along with products of spin-projection operators, products of spin–spin coupling constants also enter into the definition of the orthogonal operators $|j\rangle$. This fact also essentially distinguishes the introduced basis from the universal basis $|Knp\rangle$ given in the Introduction.

The rejection of basis universality allowed the authors of [18–23] to advance in studying the dynamics of many-body systems, at least, for some model Hamiltonians or in calculations of simpler TCFs as compared to those considered in this work.

For definiteness, consider a spin system with the Hamiltonian (2). In this case, the amplitudes $A_j(t)$ are multispin single-quantum TCFs, in which the maximum possible number of summations over lattice indices (the number of different spins) grows with increasing number j and equals $j + 1$. For $A_j(t)$, the following system of differential equations has been obtained [18–23]:

$$\dot{A}_0(t) = \nu_0^2 A_1(t),$$
$$\dot{A}_k(t) = A_{k-1}(t) - \nu_k^2 A_{k+1}(t), \quad k \geq 1. \quad (10)$$

To avoid confusion, a certain difference in the definition of amplitudes $A_j(t)$ in [18] and [19–22] should be noticed. The difference is in the factor i^j. We selected the version from [19–22], in which $A_j(t)$ contain no imaginary part, because the factor i^j is included into the definition of operators $|j\rangle$. The parameters ν_k, whose values determine the solution of the system (10), are

expressed unambiguously through moments of the NMR absorption line [18]. In particular,

$$\nu_0^2 = M_2 = \frac{9}{4}\sum_j b_{ij}^2,$$
$$\nu_1^2 = \frac{M_4 - M_2^2}{M_2}, \quad \nu_2^2 = \frac{M_2 M_6 - M_4^2}{(M_4 - M_2^2)M_2}, \tag{11}$$

where M_2, M_4, and M_6 are the second, the fourth, and the sixth moments of the NMR absorption line.

Substituting Eq. (9) into Eq. (5) yields

$$\langle n^2(t)\rangle = \sum_{j'=1}^{\infty}\sum_{j=1}^{\infty} A_{j'}(t)A_j(t)\frac{\mathrm{Tr}\{\langle j'|[S_x,[S_x,|j\rangle]]\}}{\mathrm{Tr}\{S_x^2\}}. \tag{12}$$

For crystals with a large number of nearest neighbors Z, it is possible to retain only terms with $j = j'$ in Eq. (12) when the main contribution containing the maximum possible number of summations over different lattice indices is considered. In fact, when going from operator $|j\rangle$ to operator $|j+1\rangle$, the maximum possible number of spin operators with different lattice indices entering into an orthogonal operator increases by unity. A twofold commutation with S_x does not change the number of operators but changes only their projections. For example, $S_{yi} \longrightarrow S_{zi} \longrightarrow S_{yi}$. Therefore, operators $|j\rangle$ and $|j'\rangle$ must contain the same number of spin operators for their scalar product to give a result different from zero. Note that the contribution containing terms with $j = j'$ in Eq. (12) is the only one differing from zero when only the H_{zz} part of the Hamiltonian (2) is used [24].

At the same time, contributions with a smaller number of lattice indices can also remain in the orthogonal operator for the total Hamiltonian (2) at large numbers $|j\rangle$, because, according to [18], in the process of constructing operator $|j\rangle$, operators $|j'\rangle$ with $j' < j$ are subtracted (added) with well-defined coefficients. However, these corrections are of order $(1/Z)^p$, where $p > 0$, and are small at a large number Z of neighbors [25].

Assume further that

$$\frac{\mathrm{Tr}\{\langle j|[S_x,[S_x,|j\rangle]]\}}{\mathrm{Tr}\{S_x^2\}} = \frac{F(j)\mathrm{Tr}\{\langle j|j\rangle\}}{\mathrm{Tr}\{S_x^2\}}. \tag{13}$$

Here, $F(j)$ is a certain function of j, and Eq. (13) is actually its definition. According to [18],

$$\frac{\mathrm{Tr}\{\langle j|j\rangle\}}{\mathrm{Tr}\{S_x^2\}} = \prod_{k=0}^{j-1}\nu_k^2.$$

Thus, finally, we obtain that

$$\langle n^2(t)\rangle = \sum_{j=1}^{\infty} A_j^2(t)F(j)\prod_{k=0}^{j-1}\nu_k^2. \tag{14}$$

From the stated above and Eq. (14), it is seen that the calculation of the second moment of a multiple-quantum spectrum is a very complicated many-body problem that requires a deep insight with the attraction of all the available results, including phenomenological data.

It is known that (see, for example, [21, 22]) the dependence of ν_k^2 on the number k determines the time dependences of TCFs $A_j(t)$. In this connection, further in this section, the asymptotic (at large values of time t) behavior of $\langle n^2(t)\rangle$ from Eq. (14) will be studied for several models depending on the behavior of functions ν_k^2. This study, in its turn, will allow us to select a microscopic model that can adequately describe experimental results.

To approximate functions of an integer argument $F(j)$, we will use a sum of a first-order polynomial and an oscillating function

$$F(j) = aj + c + (-1)^j(bj - c). \tag{15}$$

Equation (15) is of a rather general character, and coefficients a, b, and c in Eq. (15) can be found if operators $|j\rangle$ for the selected model are known.

Three models with the dependences $\nu_k^2 \approx \mathrm{const}$, $\nu_k^2 \approx k$, and $\nu_k^2 \approx k^2$, respectively, are considered below. The case when $\nu_k^2 \approx \mathrm{const}$ starting with a certain number k will be called the "freezing" of parameters. This situation was considered in particular in the works [20, 23], in which amplitudes $A_j(t)$ were expressed through various Bessel functions. Because the time asymptotic behavior of Bessel functions of one type is virtually similar, for the above purposes, we can use significantly simpler results obtained in [20]. Consequences following from the results of [23] will be considered additionally.

The scheme of parameter freezing proposed in [20] was based on the suggestion according to which

$$\nu_0^2 = \frac{1}{2}\mu^2, \quad \nu_j^2 = \frac{1}{4}\mu^2, \quad j \geq 1, \quad \mu = (2M_2)^{1/2}.$$

Then,

$$A_j(t) = 2^j\mu^{-j}J_j(\mu t)$$

and $\langle n^2(t)\rangle$ is expressed as follows:

$$\langle n^2(t)\rangle = 2\sum_{j=1}^{\infty} J_j^2(\mu t)F(j). \quad (16)$$

After the summation of the series [26], we obtain

$$\langle n^2(t)\rangle = c + a(\mu t)^2[J_0^2(\mu t) + J_1^2(\mu t)] - (a+b)\mu t J_0(\mu t)J_1(\mu t) - cJ_0(2\mu t). \quad (17)$$

At $\mu t \gg 1$, the substitution of asymptotic expressions for the Bessel functions in Eq. (17) gives

$$\langle n^2(t)\rangle \approx c + \frac{2a\mu t}{\pi} + \frac{a+b}{\pi}\cos(2\mu t) - \frac{c}{\sqrt{\pi\mu t}}\cos(2\mu t - \pi/4). \quad (18)$$

It is interesting to note that the linear growth of $\langle n^2(t)\rangle$ over time following from (18) was observed experimentally [7] in quasi-one-dimensional crystals of fluorapatite.

The case with a Gaussian shape of the TCF $A_0(t)$ (and, hence, with a Gaussian shape of the NMR absorption spectrum) provides an example of a linear dependence of parameters ν_k on the number

$$A_0(t) = \exp(-M_2t^2/2). \quad (19)$$

In this case,

$$\nu_k^2 = (k+1)M_2. \quad (20)$$

The NMR absorption spectrum of a Gaussian shape arises in modeling the internuclear dipole–dipole interaction using an interaction with an infinite radius (the van der Waals model). Explicit expressions for operators $|j\rangle$ and functions $A_j(t)$ in this model were found in [24]

$$A_j(t) = \frac{t^j}{j!}\exp\left(-\frac{M_2t^2}{2}\right). \quad (21)$$

Functions (21) were previously obtained in [19] with a different definition of the model. Substituting the required values of $F(j)$ in the general form (15) into Eq. (14) and carrying out the summation, we obtain

$$\langle n^2(t)\rangle = c + aM_2t^2 + (-c - M_2t^2b)\exp(-2M_2t^2). \quad (22)$$

A comparison with the exact solution obtained in [24] yields $a = 2$, $c = 1/2$, and $b = -1$. Thus, for this model, in which

$$\langle n^2(t)\rangle = \frac{1}{2} + 2M_2t^2 + \left(M_2t^2 - \frac{1}{2}\right)\exp(-2M_2t^2), \quad (23)$$

we obtain a quadratic time dependence of the growth of the second moment of the multiple-quantum spectrum. It should be noted that a linear dependence of parameters ν_k on the number can be obtained for real lattices when only the *zz*-interaction is retained in the dipole–dipole interaction (2) [27].

The dependence of parameters ν_k^2 on the number k is quadratic

$$\nu_k^2 = (k+1)(k+2)\nu_0^2, \quad (24)$$

when the TCF $A_0(t)$ is chosen in the form

$$A_0(t) = 1/\cosh^2 t. \quad (25)$$

The time in Eq. (25) is dimensionless $t \longrightarrow t(M_2/2)^{1/2}$. In this case, according to [22],

$$A_j(t) = \frac{1}{\cosh^2 t}\frac{\tanh t^j}{j!}. \quad (26)$$

Choosing $F(j)$ in the form (15) and carrying out the summation after substituting it into Eq. (14), we will find

$$\langle n^2(t)\rangle = c + 2a\sinh^2 t - c(\cosh(2t))^{-2} - 2b\sinh^2 t(\cosh(2t))^{-3}. \quad (27)$$

Equation (27) demonstrates that the growth of the second moment of a multiple-quantum spectrum over time is exponential. It was observed experimentally that the time dependence enhances with an increase in the space dimension [5, 7]. A power law was proposed for its description. Further, we will show that the experimental results reported in the recent work [9] are described well by an exponential dependence and that this shape follows from the microscopic theory. Finally, calculations using exact equations for eight moments of spectra of correlation functions [27, 28] lead to a quadratic dependence of parameters ν_k^2 on the number k in three-dimensional lattices.

TCFs in the form (25) were applied to the description of general properties of some dynamical systems in [22]. As far as we know, a function of this form was first used to describe TCFs of paramagnetic spin sys-

tems in the Blume and Hubbard's work [29]. It was obtained by solving an approximate equation derived by these authors for the autocorrelation function of the type $\mathrm{Tr}\{S_{xi}S_{xi}(t)\}/\mathrm{Tr}\{S_{xi}^2\}$ in an isotropic Heisenberg paramagnet. For nuclear spin systems coupled by the secular dipole–dipole interaction, a similar function $(1/\sinh t)$ was proposed in [30] as a trial function for the description of the nonoscillating component of NMR FID $A_0(t)$. This FID component is determined by the contribution of spins of the "long-range environment" [31].

Thus, it is evident from the above analysis that multispin processes similar to those occurring among a great number of spins of "long-range environment" and forming wings of the NMR spectrum must primarily be taken into account in order to construct a correct microscopic description [32–34]. According to [28], the exponential shape of the wing found in these works corresponds to the dependence $\nu_k^2 \propto k^2$.

4. MICROSCOPIC CALCULATION OF THE SECOND MOMENT OF A MULTIPLE-QUANTUM SPECTRUM

We will start the investigation with a consideration of systems described by the Hamiltonian (2). It was shown previously [32, 35] that the best approximation in the calculations of spin dynamics and specifically FID is obtained when the longitudinal zz-interaction is primarily taken into account while the transversal (flip–flop) interaction is taken into account to a minimum extent. Approximations of this kind are based on the axial symmetry of the Hamiltonian. This is why we may also hope for a success in the application to a more complicated four-spin TCF (8). When only the zz-contribution is retained in the Hamiltonian (2) (that is, at $a_{ij} = 0$), the quantity of our interest can readily be calculated exactly

$$\begin{aligned}\langle\langle n^2(t,\tau)\rangle\rangle_{zz} &= \sum_f \sin(b_{if}t)\sin(b_{if}\tau)\\ &\times\prod_{p\neq f}\cos(b_{ip}(t-\tau)) + 0.5\prod_p\cos(b_{fp}(t-\tau))\\ &- 0.5\prod_p\cos(b_{fp}(t+\tau))\\ &+\sum_f \sin(b_{if}t)\sin(b_{if}\tau)(P_+(t,\tau)+P_-(t,\tau)),\end{aligned} \tag{28}$$

where

$$\begin{aligned}P_\pm(t,\tau) &= \prod_{p\neq f}(\cos(b_{fp}t)\cos(b_{ip}\tau)\\ &\pm\sin(b_{fp}t)\sin(b_{ip}\tau)).\end{aligned} \tag{29}$$

Let us analyze the main properties of Eq. (28). The strong growth of the second moment in the case of time reversal ($t = \tau$) when the number of neighbors is great is provided by the first term of the autocorrelation contribution (28), which corresponds to the choice $j = f$ and $i = q$ in Eq. (8). In this case (large Z), the growth is described by the expression B^2t^2, where $B^2 = \sum_j b_{ij}^2$. This estimate is true up to the times $t^2 < (\pi/2)^2 Z/B^2$. At long times, the quadratic time dependence changes to a different one in accordance with the functional form of the dependence on the distance sufficient for the interaction between particles. Thus, for the dipole–dipole interaction of our interest ($b_{ij} \sim 1/r_{ij}^3$), the quadratic dependence will change to a linear one (see, for example, [36]). However, this is insignificant for the theory presented below, because, if the transversal interaction is taken into account at $B^2t^2 > 6$ (this condition corresponds to the time interval of the experiment [9]), the first term of the series (28) in terms of flip–flop pairs considered here will be exceeded by the second term if the condition $(\pi/2)^2 Z > 6$ is fulfilled. This condition is fulfilled already at $Z > 3$, whereas $Z = 192$ for the adamantane crystal with which the experiment [9] was performed.

The last term in the right-hand part of Eq. (28) describes the cross contribution to the second moment. In this term, the direct and reverse (time) evolutions occur at different crystal lattice sites (29), which gives rise to a lattice loop preventing the complete compensation for misphasing, which, in its turn, results in the conservation of decay. Note that the time dependence of the multiple-quantum coherence amplitudes was calculated in [37] after retaining only the term with one projection in the Hamiltonian (3). The cross contribution was not taken into account.

The contribution main for the process (first) in Eq. (28) has the structure of a star formed by bonds of the central spin i with neighbors. One of the neighbors (spin f) turns at a certain instant of time t through 180°; therefore, its contribution to the phase continues to grow upon time reversal (changing the sign of the Hamiltonian), while the contributions of all the other neighbors decrease, being completely compensated at $t = \tau$.

As the transversal term, which describes flip–flop processes in the Hamiltonian (2), is switched on, other spins f connected with the central (fixed) spin i through a chain of flip–flop processes (pairs) will also make a contribution similar to the considered one [34]. It is convenient to represent these processes with the use of diagrams. An example of two flip–flop pairs is shown in Fig. 1. The line drawn vertically designates the boundary between the direct and reverse time evolution in Eqs. (4) and (8). The vertices correspond to the dipole–dipole interaction between spins at the indicated instants of time: t_m on the left-hand side from the separating line and τ_m on the right-hand side. The integra-

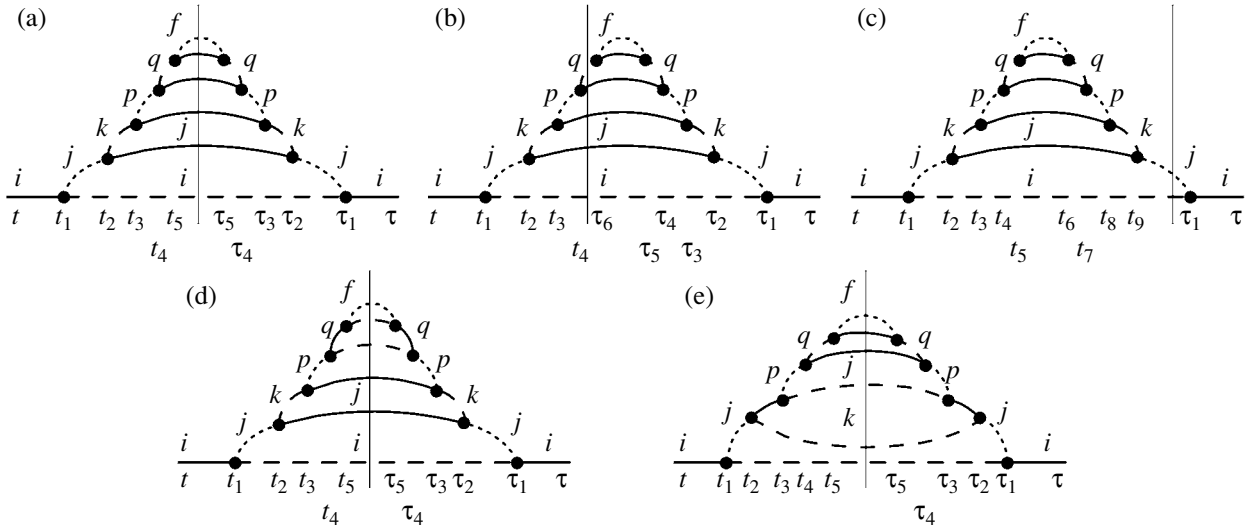

Fig. 1. Examples of diagrams for chains of two flip–flop pairs with the turned z-component of spin f entering into a longitudinal field.

tion is performed over each variable t_m (τ_m) within the limits from 0 to t_{m-1} (τ_{m-1}). Lines in the diagram correspond to the S_{xp}, S_{yp}, or S_{zp} spin components at the indicated sites i, j, f, p, etc. (spin x components are designated by solid lines; y components, by dashed lines; and z components, by dotted lines). Multiplying the dipole–dipole coupling constants corresponding to diagram vertices (Fig. 1a) together, we obtain

$$b_{ij}^2 a_{jk}^2 b_{kp}^2 a_{pq}^2 b_{qf}^2. \tag{30}$$

With the same scheme of bonds in the diagram (and with the same product of dipole–dipole coupling constants), the separating line can be located between any neighboring vertices (see Figs. 1b, 1c), which means a selection of vertices from different evolution operators in Eq. (8). The time coefficient and the sign before it depend on the location of vertices.

Consider first a situation without the turn of the fth spin (the first term $S_{xi}(t)$ in Eq. (8)) using a certain diagram with $2n$ vertices. If the two vertices at the ends of the arc of a certain spin are located on the same side from the vertical line, it is necessary to put a sign "–"; if these vertices are located on the different sides, it is necessary to put a sign "+." Let all the vertices are located on the one side from the boundary (that is, are taken from the same evolution operator). Then, these contributions have the form

$$(-1)^n \frac{t^{2n}}{(2n)!} \text{ or } (-1)^n \frac{\tau^{2n}}{(2n)!}.$$

If one vertex crosses the boundary (see, for example, Fig. 1c), the sign will change

$$-(-1)^n \frac{\tau t^{2n-1}}{(2n-1)!} \text{ or } -(-1)^n \frac{t\tau^{2n-1}}{(2n-1)!}.$$

Continuing to move vertices, we will obtain the alternating series

$$(-1)^n \sum_{m=1}^{2n} \frac{(-1)^m t^{2n-m}\tau^m}{m!(2n-m)!} = (-1)^n \frac{(t-\tau)^{2n}}{(2n)!}. \tag{31}$$

Let us pass on to the second term $\overline{S_{xi}(t)}^{(f)}$ in Eq. (8). Now, as distinct from the other vertices, the vertex corresponding to the appearance of spin f does not change its sign (more precisely, change it twice). All the difference with respect to the case considered above arises from the contribution in the situation shown in the diagram in Fig. 1a when half of vertices are located on the one side of the boundary and half, on the other side. Thus, instead of Eq. (31), we obtain

$$(-1)^n \frac{(t-\tau)^{2n}}{(2n)!} - \frac{2t^n\tau^n}{(n!)^2}. \tag{32}$$

Only the second term in (32) taken with the sign "+" remains after subtracting (32) from (31).

According to Eq. (8), diagram contributions must be summed over the lattice sites. After that, in the limit $Z \longrightarrow \infty$, we obtain the product B^6A^4 of the corresponding lattice sums rather than the product of constants (30)

$$B^2 = \sum_j b_{ij}^2, \quad A^2 = \sum_j a_{ij}^2. \tag{33}$$

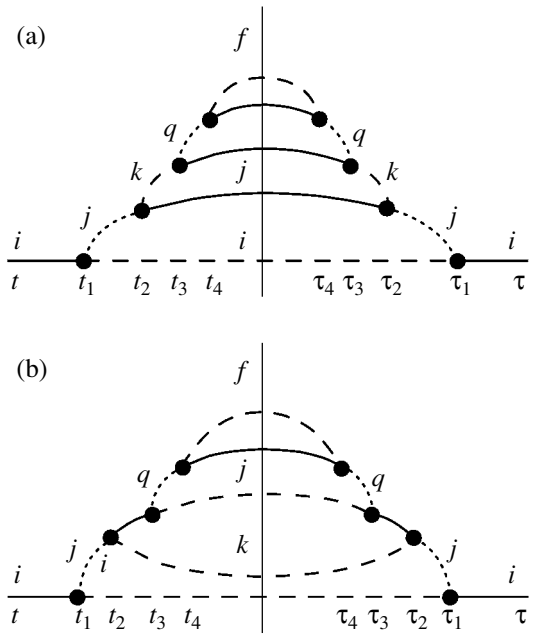

Fig. 2. Examples of diagrams for chains of two flip–flop pairs with the turned y-component of spin f entering into the second flip–flop pair.

Let us return to the diagrams under consideration. As an example, the yy-interaction is used in Fig. 1a for pairs participating in flip–flop processes. In a different example presented in Fig. 1d, the xx-interaction is used in the second pair. To obtain the final answer taking into account all the possible realizations of flip–flop processes, these diagrams should be summed, which evidently results in a factor of 2 for each flip–flop pair. Eventually, in each flip–flop pair, we can couple the subsequent chain to the first rather than second spin, as it is shown in Fig. 1e (with the example of the first flip–flop pair). The enumeration of possible variants leads to another factor of 2 for each flip–flop pair.

Summing all these chains containing different numbers of flip–flop pairs leads to the following result for the contribution with the topology indicated in diagrams in Fig. 1:

$$\begin{aligned}\langle n^2(t)\rangle_{zd}^{(0)} &= \sum_{m=1}^{\infty} B^2(4B^2A^2)^{m-1}t^{4m-2}/((2m-1)!)^2 \\ &= \frac{B}{4A}[I_0(y)-J_0(y)],\end{aligned} \tag{34}$$

where $I_0(y)$ and $J_0(y)$ are Bessel functions, and $y^2 = 8ABt^2$.

In the lowest approximation with respect to flip–flop processes, in addition to diagrams shown in Fig. 1 and corresponding to the occurrence of the chosen spin f as the z-projection of the field, the similar contribution will be made by diagrams with the similar topology of the chain corresponding to the occurrence of the y-component of the chosen spin f in the last flip–flop pair of the chain. Examples of such diagrams with two flip–flop pairs are shown in Fig. 2. Such diagrams with the y-component of the chosen spin f in the last flip–flop pair can also be formed when this pair is connected by the xx-bond to the z-component of spin f at the end of the chain. This will lead to the doubling of the amplitude before contributions in Eq. (34). (Such a contribution was not taken into account in diagrams with a finite z-field of spin f, because field fluctuations were not taken into account there). Repeating the same considerations as in the previous case (34), we will write

$$\begin{aligned}\langle n^2(t)\rangle_{yd}^{(0)} &= 0.5\sum_{m=1}^{\infty}\frac{(4B^2A^2)^m t^{4m}}{((2m)!)^2} \\ &= \frac{1}{4}[I_0(y)+J_0(y)-2].\end{aligned} \tag{35}$$

The value of y was determined above.

The complete expression for the required function is obtained by summing expressions (34) and (35). Because the Bessel functions $I_0(y)$ exhibit an exponential asymptotic behavior at large values of their argument y, an exponential growth over time is obtained

$$\langle n^2(t)\rangle_{d}^{(0)} \sim \exp(yt).$$

The above consideration demonstrates that summing the indicated 0–f chains provides a fast growth of $\langle n^2(t)\rangle$. The interaction of chain spins with the environment will retard this growth. To estimate this effect, we will use a simple but effective approximation [32, 35] and will dress lines corresponding in the considered diagrams to the transversal spin projections with the longitudinal zz-interaction. Now, as well as in Eq. (28), each line will correspond to a product of cosines replaced by a Gaussian function at large Z

$$\begin{aligned}g(t_{2k}-\tau_{2k}) &= \prod_j \cos(b_{ij}(t_{2k}-\tau_{2k})) \\ &\approx \exp\left\{-\frac{(t_{2k}-\tau_{2k})^2B^2}{2}\right\}.\end{aligned} \tag{36}$$

At complete symmetry of the arguments $t_{2k} = \tau_{2k}$, the decay disappears. However, integration breaks the sym-

metry, and the decay decreases the value of the integral

$$\int_0^t dt_2 \int_0^{t_2} dt_4 \ldots \int_0^{t_{2m-2}} dt_{2m} \int_0^{\tau} d\tau_2$$

$$\times \int_0^{\tau_2} d\tau_4 \ldots \int_0^{\tau_{2m-2}} d\tau_{2m} (t - t_2) \ldots (t_{2m-2} - t_{2m}) \quad (37)$$

$$\times t_{2m} (\tau - \tau_2) \ldots (\tau_{2m-2} - \tau_{2m}) \tau_{2m}$$

$$\times g^2(t_2 - \tau_2) \ldots g^2(t_{2m} - \tau_{2m}) g(t - \tau)$$

as compared to its value

$$t^{2m+1} \tau^{2m+1} / ((2m+1)!)^2$$

from (34). Here, the specificity of "dressing" the transversal lines with the *zz*-interaction was taken into account. The result of dressing does not depend on the positions of vertices with odd numbers (see Fig. 1) also corresponding to the *zz*-interaction. Therefore, integration over variables t_{2k+1} and τ_{2k+1} was performed in (37).

To estimate the possible value of the decrease in the integral, we replace $g^2(t_{2k} - \tau_{2k})$ with a δ-function

$$g^2(t_{2k} - \tau_{2k}) = \delta(t_{2k} - \tau_{2k}) T.$$

Here, $T = \pi^{1/2}/B$ is the integral of the Gaussian function. After this replacement, the integration over variables τ_2, …, τ_{2m} is excluded. Performing integration over variables t_2, …, t_{2m}, we find that

$$\langle n^2(t) \rangle_{zd}^{(1)} = \sum_{m=0}^{\infty} \frac{2^{m+1} T^m B^2 (4B^2 A^2)^m t^{3m+2}}{(3m+2)!}$$

$$= \frac{1}{6} \left(\frac{B}{TA^2} \right)^{2/3} \left\{ e^x - 2e^{-x/2} \cos\left(\frac{\sqrt{3}x}{2} - \frac{\pi}{3} \right) \right\}, \quad (38)$$

where

$$x = 2t(A^2 B^2 T)^{1/3} = 2t(A^2 B / 2\sqrt{\pi})^{1/3}.$$

Similarly, after taking into account the decay in the case of (35), we obtain

$$\langle n^2(t) \rangle_{yd}^{(1)} = 0.5 \sum_{m=1}^{\infty} \frac{2^m T^m (4B^2 A^2)^m t^{3m}}{(3m)!}$$

$$= \frac{1}{6} \left(e^x + 2e^{-x/2} \cos \frac{\sqrt{3}x}{2} \right) - 0.5. \quad (39)$$

The value of x was determined above. The complete expression for the required function $\langle n^2(t) \rangle$ is obtained by summing expressions (38) and (39).

Thus, the decay of correlations decreased the exponent in the dependence $\langle n^2(t) \rangle$ by a factor of $y/x = (8B/\pi A)^{1/6}$. For the dipole–dipole interaction ($B = 2A$), this leads to retardation by a factor of 1.31. It is clear that retardation will be enhanced if the dressing of *z*-lines with transversal interactions is performed.

Let us now pass on to systems with the effective Hamiltonian (3). In this case, the simplest chain between the initial spin and the flipped spin *f* is constructed by alternating the *zz*- and *yy*-interactions, for example, as in the diagrams presented in Figs. 1a–1c and Fig. 2a. The selection of the first bond connected to S_{xi} predetermines the rest. The combinatorial factor equals 2, because there are only two possibilities: the case of *zyzyzy*… diagrams considered above or the case of *yzyzyz*… diagrams obtained from the preceding ones by substituting *z*-lines for *y*-lines and vice versa. However, the chain can be constructed in a different way. The *zz*- or *yy*-bonds in the *j*th link can be connected to the operator S_{xj} (see Fig. 1e or Fig. 2b). Enumerating all such possibilities, we obtained the following combinatorial factor for a chain of *m* links (see Appendix):

$$N_m = \frac{2}{3}(2^m - (-1)^m). \quad (40)$$

Having performed a summation over all such chains, we write the time series

$$\langle n^2(t) \rangle_{\text{eff}}^{(0)} = \sum_{m=1}^{\infty} \frac{N_m (C^2 t^2)^m}{(m!)^2}$$

$$= \frac{2}{3}[I_0(z) - J_0(2Ct)], \quad (41)$$

where

$$z^2 = 8C^2 t^2 \text{ and } C^2 = \sum_j c_{ij}^2.$$

Now, we will take into account the effect of the interaction of chain spins with the environment on the growth of $\langle n^2(t) \rangle_{\text{eff}}$. Because the Hamiltonian (3) has no axial symmetry, all the lines in the chain diagrams should be dressed to the corresponding autocorrelation functions $\Gamma_x(t)$ or $\Gamma_y(t) = \Gamma_z(t)$. This leads to a very complicated multiple integrals over interlocked time variables. The following simplifications will be made to estimate the effect:

(1) in chain diagrams having the ladder form, we will dress only segments in lateral lines and will leave steps (bridges) undressed;

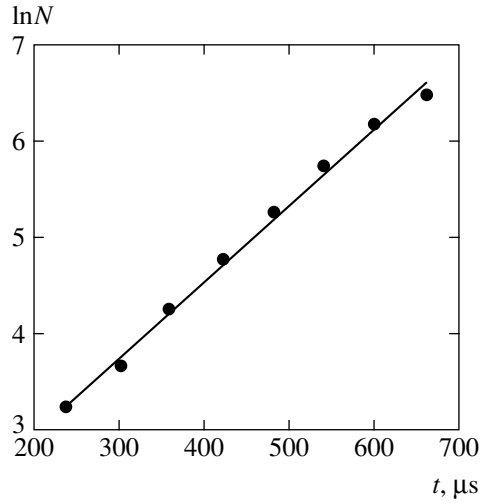

Fig. 3. Dependence of the number of correlated spins on the preparation time. Points are experimental data for adamantane from [9]. The straight line corresponds to Eq. (47).

(2) instead of functions $\Gamma_x(t)$ or $\Gamma_y(t) = \Gamma_z(t)$ whose second moments differ by a factor of 2 ($2C^2$ and C^2), we will take one function $\Gamma(t)$ in the form of a Gaussian function with the averaged second moment $M_{2c} = 5C^2/4$ (the averaging is performed with regard to the alternation of projections of spin operators in the sequence of chain links considered in the Appendix, according to which the total second moment of the side line of a chain of m links changes from mC^2 for the simplest chain to $3mC^2/2$ for a chain with the maximum number $m/2$ of simplest sections);

(3) the contributions of the right-hand and left-hand side lines corresponding to two sections of evolution in (3) will be estimated independently; that is, we will consider that

$$\langle\langle n^2(t, \tau)\rangle\rangle_{\text{eff}}^{(1)} \propto G(t)G(\tau). \tag{42}$$

With regard for the above assumptions, the function $G(t)$ is determined by the series in terms of the number of segments in the side line

$$G(t) = \sum_{m=1}^{\infty} \omega_c^m \int_0^t dt_1 \int_0^{t_1} dt_2 \ldots \int_0^{t_{m-1}} dt_m \Gamma(t - t_1)\ldots\Gamma(t_{m-1} - t_m)\Gamma(t_m), \tag{43}$$

where $\omega_c = C\sqrt{2}$ is the mean interaction per one vertex obtained on the basis of a comparison of (42) and (41). The series (43) is readily summed after carrying out the Laplace transformation. For the Laplace transform of the function $G(t)$, we find that

$$L_G(p) = \frac{\omega_c w(p)}{1 - \omega_c w(p)}, \tag{44}$$

where $w(p)$ is the Laplace transform of the Gaussian function, which is the probability integral with a complex argument whose values are given in the book [38]. The behavior of the function $G(t)$ at long times of our interest is determined by the nearest root of the denominator in the right-hand part of Eq. (44). Thus, we find that

$$p_{\min} = 0.47\sqrt{2M_{2c}}, \quad G(t) \approx \exp(0.743Ct). \tag{45}$$

Finally, substituting the values from (45) to expression (42), we obtain the required estimate

$$\langle n^2(t)\rangle_{\text{eff}}^{(1)} \approx \exp(1.486Ct) = \exp(0.5\sqrt{M_2}t). \tag{46}$$

A comparison with the exponent $2Ct\sqrt{2}$ of the time asymptotic form of Eq. (41) shows that the exponent decreased by a factor of 1.9 after taking into account the decay of correlations.

The above analysis explains how the rotation by an angle φ about the x axis combined with the direct and reverse evolution stages in (4) brings the expression for $\langle n^2(t)\rangle$ to a series in terms of time powers with positive coefficients rather than a conventional alternating series for autocorrelation functions or FID. For a large number of neighbors, we managed to sum the main part of this series—trees in the form of dressed chains—and obtain an exponential growth of $\langle n^2(t)\rangle$. Thus, we see a full agreement with the result (27) obtained using an expansion of correlation function (5) in terms of orthogonal operators.

Let us make some concluding remarks concerning the theoretical model considered here. Note that, besides the autocorrelation contribution with $j = f$ and $i = q$ in (8), a different set of indices can be selected. In this case, only a small number of terms will change quantitatively, which will not affect the qualitative behavior of infinite series.

It follows from Eq. (28) that the zz-interaction for a small number Z of neighbors gives rise to oscillations rather than the growth of the second moment of multiple-quantum NMR $\langle n^2(t, t)\rangle \propto B^2t^2$, which is characteristic of this model in the case of large Z. Similar oscillations of the amplitudes of multiple-quantum coherences are also observed in the one-dimensional xy-model [39]; however, Bessel functions rather than ordinary cosines arise there. The occurrence of oscillations is a consequence of multiple acts of interaction between the same neighbors. On the other hand, the value of $1/Z$ is small at a large number of neighbors; therefore,

repeated interactions can be neglected, which leads to a monotonic growth of the second moment over time.

5. COMPARISON WITH EXPERIMENT

The growth of the number of spins involved in a correlated motion over time was studied by multiple-quantum NMR spectroscopy in many experimental works. The behavior of the currently greatest number of correlated spins (650) was studied in adamantane in the recently published work [9], in which evolution with the Hamiltonian (3) was observed. Because the distribution of intensities in the multiple-quantum spectrum was found to be close to the normal one (1), the second moment of the distribution was determined using a Gaussian function with a close width. To be precise, the quantity $K = N(t) = 2\langle n^2(t)\rangle$, which was called the number of correlated spins, was considered. The time dependence of this quantity is shown in Fig. 3 in semilogarithmic coordinates. The results are described well by the dependence

$$N(t) = A_e \exp(a_e t) \tag{47}$$

with the parameters found by the least-squares method

$$A_e = 4.0, \quad a_e = 0.0079\ \mu s^{-1} = 0.3(M_2)^{1/2}. \tag{48}$$

To obtain the dimensionless value in (48), we used the theoretical value of the second moment of the adamantane NMR absorption spectrum $(M_2)^{1/2} = 4.19$ kHz calculated in [5]. The experimental value of M_2 was not reported in [9]; however, it can be judged from the reported FID that it is close to the theoretical one.

Our estimate for the exponent in (46) exceeds the value of a_e in (48) by a factor of 1.65. Probably, this primarily points to the fact that the decay of correlations has not been taken into account to a sufficient accuracy with the assumed approximations. However, a certain contribution to the value of this ratio can also be made by the deviation of the intensity distribution from the Gaussian function.

6. DISCUSSION OF THE RESULTS

The present study relates the time dependence of the second moment $\langle n^2(t)\rangle$, which characterizes the number of correlated spins, to properties of the spin system. The fastest exponential grows is exhibited by systems with a great number of neighbors, in the description of which the correlation of contributions of different neighbors to the local field arising on a third spin can be neglected. In this case, trees make the main contribution in the time series for $\langle n^2(t)\rangle$ if the interaction has a sufficiently general form. We obtained an exponential dependence by two methods: firstly, by summing the dressed chains in the time series for $\langle n^2(t)\rangle$ and, secondly, by expanding the correlation functions (5) in terms of orthogonal operators. The case of trees indicated above corresponds to a quadratic growth of parameters ν_k^2 as functions of number. A comparison with the experiment clearly demonstrates that real three-dimensional systems can be assigned to the systems of the above type.

For systems with an Ising-type Hamiltonian, that is, for systems whose Hamiltonian contains the interaction only between spin projections of one kind, the time dependence $\langle n^2(t)\rangle$ weakens to a power dependence: $\langle n^2(t)\rangle \propto t^2$. Star-shaped diagrams, which constitute a small part of all trees, remain in the time series for $\langle n^2(t)\rangle$ in this case. Parameters ν_k^2 of the expansion in terms of orthogonal operators grow linearly as functions of number.

Even a weaker dependence $\langle n^2(t)\rangle \propto t$ was obtained for one-dimensional systems. Parameters ν_k^2 of the expansion in terms of orthogonal operators become independent of the number (become frozen), and only simple (undressed) chains (without summing over the lattice) remain among the diagrams.

The enhancement of the growth law for the number of dynamically correlated spins with increasing space dimension followed from the theory proposed previously in [5]. The main approximation used in this theory is the assumption that the cluster of correlated spins is dense and grows only at the surface. Because the fraction of spins on the surface with respect to the total number of spins decreases with decreasing space dimension, the growth rate decreases.

The formation of a dense cluster means the occurrence of a collective, strongly correlated motion of spins. On the contrary, the results presented above suggest an increase in the number of dynamically correlated spins while the interactions of a spin with each of its neighbors remain independent. As a result, the proposed theory implies a stronger (exponential rather than power) growth of $N(t)$ over time. Of course, interactions with neighbors in three-dimensional systems must actually be correlated to a certain extent; however, this correlation must not be as strong as in the theory proposed in [5]. For example, taking into account the correlation of contributions of different neighbors to the local field on a third spin leads to an increase in the coordinate of the singularity of time correlation functions by 10–20% [33, 34].

ACKNOWLEDGMENTS

The authors are grateful to F.S. Dzheparov for a discussion of the results and useful comments.

APPENDIX

The simplest chain between the initial spin and the flipped spin f for systems described by Hamiltonian (3) is constructed by alternating the zz- and yy-interactions.

The selection of the first bond connected to S_{xi} predetermines the rest. In the general case, the combinatorial factor for a chain composed of q simple sections will be equal to 2^q. To find the total number N_m of different chains of m links, 2^q of similar factors should be considered and summed for all possible partitions of the number of links between q sections under the condition that

$$m = \sum_{i=1}^{q} m_i.$$

To perform this operation, we introduce generating functions of the required numbers, the numbers of simple chains (end sections), and the numbers of inner sections, respectively,

$$F = \sum_{m=1}^{\infty} N_m \theta^m,$$

$$F_1 = \sum_{m=1}^{\infty} 2\theta^m = \frac{2\theta}{1-\theta}, \text{ and } F_2 = \sum_{m=2}^{\infty} 2\theta^m = \frac{2\theta^2}{1-\theta},$$

where θ is a formal parameter. Based on the above rules for the construction of chains, we obtain that

$$F(\theta) = \sum_{q=0}^{\infty} (F_2(\theta))^q F_1(\theta)$$

$$= \frac{F_1(\theta)}{1-F_2(\theta)} = \frac{2\theta}{(1+\theta)(1-2\theta)}.$$

Hence, multiplying together two series in terms of powers of θ, we find the required Eq. (40) for the coefficient before θ^m.

REFERENCES

1. R. Balescu, *Equilibrium and Nonequilibrium Statistical Mechanics* (Wiley, New York, 1975; Mir, Moscow, 1978), Vol. 2.
2. J. Baum, M. Munovitz, A. N. Garroway, and A. Pines, J. Chem. Phys. **83**, 2015 (1985).
3. M. Munovitz and A. Pines, Adv. Chem. Phys. **6**, 1 (1987).
4. R. R. Ernst, G. Bodenhausen, and A. Wokaun, *Principles of Nuclear Magnetic Resonance in One and Two Dimensions* (Clarendon, Oxford, 1987; Mir, Moscow, 1990).
5. D. H. Levy and K. K. Gleason, J. Phys. Chem. **96**, 8126 (1992).
6. S. Lacelle, S. Hwang, and B. Gerstein, J. Chem. Phys. **99**, 8407 (1993).
7. G. Cho and J. P. Yesinowski, J. Chem. Phys. **100**, 15716 (1996).
8. C. Ramanathan, H. Cho, P. Cappellaro, et al., Chem. Phys. Lett. **369**, 311 (2003).
9. H. G. Krojanski and D. Suter, Phys. Rev. Lett. **93**, 090501 (2004).
10. H. Cho, T. D. Ladd, J. Baugh, et al., Phys. Rev. B **72**, 054427 (2005).
11. J.-S. Lee and A. K. Khitrin, Phys. Rev. Lett. **94**, 150504 (2005).
12. J.-S. Lee and A. K. Khitrin, J. Chem. Phys. **122**, 041101 (2005).
13. R. H. Schneder and H. Schmiedel, Phys. Lett. A **30**, 298 (1969).
14. W. K. Rhim, A. Pines, and J. S. Waugh, Phys. Rev. B **3**, 684 (1971).
15. A. K. Khitrin, Chem. Phys. Lett. **274**, 217 (1997).
16. A. Abragam, *The Principles of Nuclear Magnetism* (Clarendon, Oxford, 1961; Inostrannaya Literatura, Moscow, 1963), Chap. 4.
17. U. Haeberlen, *High Resolution NMR in Solids* (Academic, New York, 1976; U. Haeberlen and M. Mehring, Mir, Moscow, 1980).
18. F. Lado, J. D. Memory, and G. W. Parker, Phys. Rev. B **4**, 1406 (1971).
19. M. H. Lee, Phys. Rev. Lett. **52**, 1579 (1984).
20. M. H. Lee and J. Hong, Phys. Rev. B **32**, 7734 (1985).
21. J. M. Liu and G. Müller, Phys. Rev. A **42**, 5854 (1990).
22. M. H. Lee, I. M. Kim, W. P. Cummings, and R. Dekeyser, J. Phys.: Condens. Matter **7**, 3187 (1995).
23. V. L. Bodneva, A. A. Lundin, and A. A. Milyutin, Teor. Mat. Fiz. **106**, 370 (1996).
24. V. E. Zobov and A. A. Lundin, Teor. Mat. Fiz. **141**, 1737 (2004).
25. A. A. Lundin and V. E. Zobov, J. Magn. Reson. **26**, 229 (1977).
26. A. P. Prudnikov, Yu. A. Brychkov, and O. I. Marichev, *Integrals and Series. Special Functions* (Nauka, Moscow, 1983; Gordon and Breach, New York, 1986), Sect. 5.7.11.
27. J. Jensen, Phys. Rev. B **52**, 9611 (1995).
28. M. Böhm, H. Leschke, M. Henneke, et al., Phys. Rev. B **49**, 5854 (1994).
29. M. Blume and J. Hubbard, Phys. Rev. B **1**, 3815 (1970).
30. M. Engelsberg and I. J. Lowe, Phys. Rev. B **10**, 822 (1974).
31. A. A. Lundin and B. N. Provotorov, Zh. Éksp. Teor. Fiz. **70**, 2201 (1976) [Sov. Phys. JETP **43**, 1149 (1976)].
32. A. A. Lundin, A. V. Makarenko, and V. E. Zobov, J. Phys.: Condens. Matter **2**, 10131 (1990).
33. V. E. Zobov and M. A. Popov, Zh. Éksp. Teor. Fiz. **124**, 89 (2003) [JETP **97**, 78 (2003)].
34. V. E. Zobov and M. A. Popov, Teor. Mat. Fiz. **136**, 463 (2003).
35. V. E. Zobov and A. A. Lundin, Zh. Éksp. Teor. Fiz. **106**, 1097 (1994) [JETP **79**, 595 (1994)].
36. F. S. Dzheparov, A. A. Lundin, and T. N. Khazanovich, Zh. Éksp. Teor. Fiz. **92**, 554 (1987) [Sov. Phys. JETP **65**, 314 (1987)].
37. A. K. Khitrin, JETP **82**, 1172 (1996).
38. *Handbook of Mathematical Functions*, Ed. by M. Abramowitz and I. A. Stegun, 2nd ed. (Dover, New York, 1972; Nauka, Moscow, 1979).
39. S. I. Doronin, I. I. Maksimov, and E. B. Fel'dman, Zh. Éksp. Teor. Fiz. **118**, 687 (2000) [JETP **91**, 597 (2000)].

Translated by A. Bagaturyants